Computational Study of Edge Configuration and Quantum Confinement Effects on Graphene Nanoribbon Transport

Sako, Ryutaro
Hosokawa, Hiroshi
Tsuchiya, Hideaki

(Citation)
IEEE Electron Device Letters,32(1):6-8

(Issue Date)
2011-01

(Resource Type)
journal article

(Version)
Accepted Manuscript

(URL)
https://hdl.handle.net/20.500.14094/90001273

Computational Study of Edge Configuration and Quantum Confinement Effects on Graphene Nanoribbon Transport

Ryūtaro Sako, Hiroshi Hosokawa, and Hideaki Tsuchiya, *Senior Member*, *IEEE*

***Abstract*—We investigated edge configuration and quantum confinement effects on electron transport in armchair-edged graphene nanoribbons (A-GNRs), by using a computational approach. We found that the edge bond relaxation has a significant influence not only on the band-gap energy, but also on the electron effective mass. We also found that A-GNRs with $N = 3m$ family (N is number of atoms in its transverse direction and m a positive integer) exhibits smaller effective mass, by comparing at the same band-gap energy. As a result, A-GNRs with $N = 3m$ family are found to be favorable for use in channels of field-effect transistors.**

***Index Terms*—graphene nanoribbon, edge bond relaxation, quantum confinement, band-gap, effective mass, ballistic transport**

I. Introduction

With the scaling limit of Si field-effect transistors (FETs) in sight, there has been a persistent pursuit for alternative device structures and materials that could outperform the conventional Si FETs [1]. Because of promising progress on fabricating and patterning a graphene layer on ordinary device setups, graphene electronics has been a topic of extensive research interests [2]. A narrow strip of graphene, that is, graphene nanoribbon (GNR), has the ability to tune the band-gap, depending on its structure and ribbon width [3]-[6]. In theory, it has been demonstrated that armchair-edged GNRs (A-GNRs) exhibit larger band-gaps than those of a bilayer graphene (BLG) under a vertical electric field [7]-[9], and furthermore A-GNR-FETs have, in principle, higher performance potentials than those of BLG-FETs [9].

Since A-GNRs are geometrically terminated single graphene layers and the band-gaps originate from quantum confinement, their electronic structures are crucially influenced by edge configurations [7], [10], [11]. In fact, previous first-principles simulations indicated that the edge bond relaxation in A-GNRs plays an important role in determining their band-gap energies, because the bonding characteristics between carbon atoms abruptly change at the edges [7]. However, its influence on electron transport has been ill-argued, except a computational study of A-GNR tunneling-FETs [11]. So, we address the subject in this paper and clarify the edge configuration and quantum confinement effects on electron transport in A-GNRs based on a computational approach. The electrical characteristics of A-GNR-FETs considering those effects are also discussed by using a top-of-the-barrier ballistic MOSFET model [12].

Manuscript received August, 2010.

The authors are with the Department of Electrical and Electronics Engineering, Graduate School of Engineering, Kobe University, 1-1, Rokko-dai, Nada-ku, Kobe 657-8501, Japan (e-mail: 0734331t@stu.kobe-u.ac.jp, 102t258t@stu.kobe-u.ac.jp, tsuchiya@eedept.kobe-u.ac.jp). This work was supported by the Semiconductor Technology Academic Research Center (STARC).

II. Approach

We compute the electronic bandstructures of A-GNRs using a tight-binding (TB) approach, where a TB Hamiltonian with a p_z orbital basis set is used. One p_z orbital per atom is enough for atomistic physical description since s, p_x, and p_y are far from the Fermi level and do not play an important role for electron transport. A p_z orbital hopping integral of $\gamma_0 = 2.6$ eV is used [8], and only the nearest neighbor coupling is considered. All carbon-carbon bond lengths are taken as 0.142 nm, except for those carbon-carbon bonds at the edges. Because previous first-principles relaxation calculations [7] have indicated that carbon-carbon bonds at the edges, which are also bonded to hydrogen atoms to terminate dangling bonds, are about 3.5 % shorter than other carbon-carbon bonds inside the ribbon. Therefore, these bond lengths have been determined to be 0.137 nm. Further, to fit the first-principles bandstructure results, we used a different TB parameter of $\gamma_0' = 1.12\ \gamma_0$ for the edge bonds [7], [11]. Here, we add that the band-gap underestimation problem well-known for first-principles simulations based on the density-functional theory (DFT) is much less serious for GNRs because the band-gap of GNRs is caused by quantum confinement of the gapless p_z orbital bands of graphene, which is well described by the DFT, unlike the band-gap originating from lattice potential as in Si [13].

III. Electronic Bandstructures

We first examine the effect of edge bond relaxation on the band-gap and the electron effective mass. Figs. 1 and 2 show the band-gap energy and the electron effective mass as a function of ribbon width, respectively. The effective mass was calculated by performing a second order differential of the E-k dispersion relation for the first conduction subband minimum with respect to wave number. Here, (a) and (b) correspond to

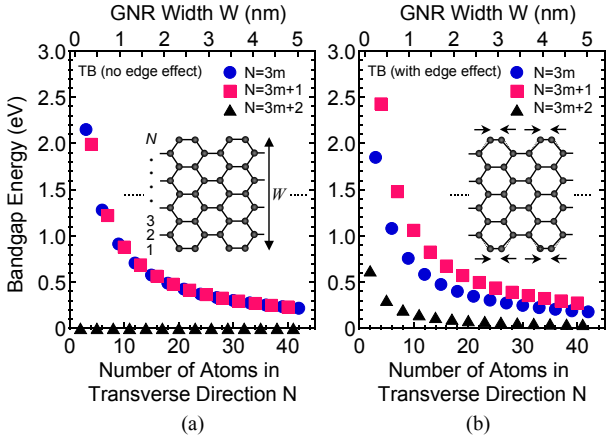

Fig. 1. Band-gap energy as a function of ribbon width, where (a) and (b) correspond to the results without and with the presence of edge bond relaxation, respectively. m in the legend represents a positive integer. The lower and upper horizontal axes denote number of carbon atoms in transverse direction N and actual ribbon width W in unit of nm, respectively. The insets depict the atomic models of A-GNRs used in the simulation. Note that in (b) the carbon-carbon bond lengths at the edges are shortened by about 3.5% as compared to other carbon-carbon bonds inside the ribbon.

the results without and with the presence of edge bond relaxation, respectively. The insets in Fig. 1 depict the atomic models of A-GNRs used in the simulation. Note that in (b) the carbon-carbon bond lengths at the edges are shortened by about 3.5 % as compared to other carbon-carbon bonds inside the ribbon. As reported in [7], the edge bond relaxation has a significant influence on the band-gap as shown in Fig. 1. In fact, without the edge bond relaxation, A-GNRs are metallic if $N = 3m + 2$ (where m is a positive integer), or otherwise it is semiconducting as shown in Fig. 1 (a). However, when the edge bond relaxation is considered, there are no metallic nanoribbons and furthermore the band-gaps are well separated into three different groups, as shown in Fig. 1 (b). Such a change in the band-gap hierarchy mentioned above has been attributed to the 12 % increase of the hopping integrals between carbon atoms at the edges, that is, $\gamma_0' = 1.12\ \gamma_0$ for the edge bonds [7].

Next, as shown in Fig. 2 the edge bond relaxation has also a significant influence on the electron effective mass, where the results for $N = 3m + 2$ are omitted in Fig. 2 because effective mass can not be defined in that case due to their linear dispersion relation. Due to the edge bond relaxation, the effective mass decreases in $3m$ A-GNRs, and by contraries increases in $(3m + 1)$ A-GNRs as shown in Fig. 2 (b). Consequently, $3m$ A-GNRs seem to be favorable for use in channels of FETs. However, the band-gap energy also decreases (increases) in $3m$ A-GNRs [$(3m + 1)$ A-GNRs] as shown in Fig. 1 (b), so a comparison of the transport properties under the same band-gap energy becomes important in terms of the FET application. To this end, we focus on two pairs of A-GNRs with $N = 6$ and 10, which have $E_G \sim 1.1$ eV, and A-GNRs with $N = 12$ and 19, which have $E_G \sim 0.6$ eV. Fig. 3 shows the bandstructures computed for the two pairs of A-GNRs, where the edge bond relaxation is considered. It is

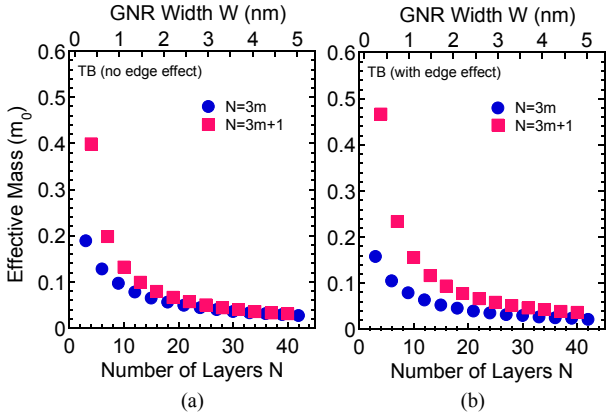

Fig. 2. Effective mass at conduction band minimum as a function of ribbon width, where (a) and (b) correspond to the results without and with the presence of edge bond relaxation, respectively. Note that the results for $N = 3m + 2$ are omitted because effective mass can not be defined in that case due to their linear dispersion relation.

found that the A-GNRs with $N = 3m$ family have a steeper slope than those with $N = 3m + 1$ family, though almost the same band-gap energies are created. As a result, smaller effective masses are obtained for $N = 3m$ family even under the condition of the same band-gap energy. They are $m = 0.105\ m_0$ ($0.156\ m_0$) for $N = 6$ ($N = 10$), and $0.064\ m_0$ ($0.078\ m_0$) for $N = 12$ ($N = 19$). We will discuss electrical characteristics of A-GNR-FETs, by fully considering the atomistic bandstructures in the next section.

IV. Electrical Characteristics

To directly examine influences of the atomistic bandstructures on the device performances, we compute the electrical characteristics under ballistic transport based on a "top-of-the-barrier" model [12]. The model has been proven to be suitable for a systematic study comparing the performance limits of atomistic transistors including carbon-based FETs [13]-[15]. Comparison to the detailed quantum simulations based on the non-equilibrium Green's function method demonstrated that the model is valid for the MOSFET structure if the channel length is larger than 10 nm, because quantum tunneling is not considered [16]. Fig. 4 shows the schematic diagram of the simulated GNR-FETs, where the source and drain are assumed to be heavily doped GNR contacts while the

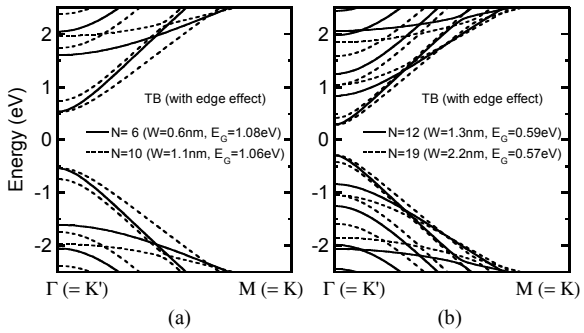

Fig. 3. Bandstructures of A-GNRs with (a) $N = 6$ and 10 ($E_G \sim 1.1$ eV), and (b) $N = 12$ and 19 ($E_G \sim 0.6$ eV).

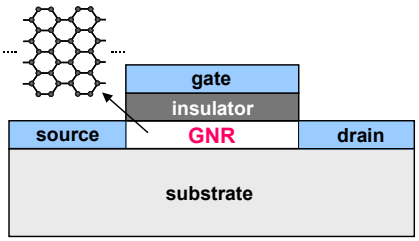

Fig. 4. Schematic diagram of the simulated GNR-FETs, where the source and drain are assumed to be heavily doped GNR contacts while the channel is intrinsic. The gate insulator was assumed to be SiO_2.

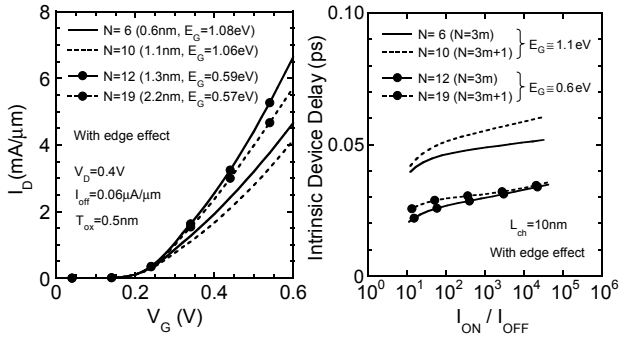

Fig. 5. (a) I_D-V_G characteristics and (b) intrinsic device delays versus I_{ON} / I_{OFF} ratio for N=6, 10, 12 and 19. V_D = 0.4 V and T_{ox} = 0.5 nm. In (a), the simulations are performed at the same OFF-current density (I_{off} = 0.06μA/μm). In (b), the channel length is assumed to be 10 nm. Temperature is 300K.

channel is intrinsic. Fig. 5 shows (a) the drain current versus gate voltage (I_D - V_G) characteristics and (b) the intrinsic device delays versus the ON-OFF current ratio, where the intrinsic device delay is calculated as $\tau = (Q_{ON} - Q_{OFF}) / I_{ON}$, where Q_{ON} and Q_{OFF} are the total charge in the channel at on-state and off-state, respectively, and I_{ON} is the on-current. The gate insulator (SiO_2) thickness is T_{ox} = 0.5 nm and temperature is 300 K. The drain voltage is set sufficiently small (V_D = 0.4 V), thus band-to-band tunneling is ignored in this study. Here, to make a reasonable comparison between different device architectures, we used a technique to consider both the on-state and off-state at the same power supply voltage in Fig. 5 (b), where the curves were obtained by sweeping a constant V_{DD} (= 0.4V)-bias window along V_G axis in the I_D - V_G characteristics [17]. As expected from the difference in the bandstructures between $N = 3m$ and $3m + 1$ families mentioned before, the drain current (the delay) is always larger (smaller) in the $N = 3m$ family, if the same band-gap FETs are compared. Similar results have been obtained for a thicker gate insulator with T_{ox} = 1.5 nm (The results are not shown here). Therefore, A-GNR-FETs with $N = 3m$ family are preferable as a high-performance digital switch in future logic circuits.

V. Conclusion

We investigated the influences of edge bond relaxation and quantum confinement effects on electron transport in armchair-edged graphene nanoribbons, by using a computational approach based on the atomistic TB bandstructure calculation and ballistic transport model. We found that the edge bond relaxation has a significant influence not only on the band-gap opening due to the quantum confinement, but also on the determination of electron effective mass. In particular, the edge bond relaxation was found to decrease (increase) the electron effective mass of $3m$ A-GNRs [$(3m + 1)$ A-GNRs]. Thus, we further performed a ballistic MOSFET simulation using the atomistic bandstructures, and demonstrated that $3m$ A-GNRs exhibit superior device performances over $(3m + 1)$ A-GNRs, in principle.

References

[1] ITRS, International Technology Roadmap for Semiconductors. [Online]. Available: www.itrs.net

[2] K.S. Novoselov, A.K. Geim, S.V. Morozov, D. Jiang, Y. Zhang, S.V. Dubonos, I.V. Grigorieva, and A.A. Firsov, "Electric field effect in atomically thin carbon films," *Science*, vol. 306, pp. 666-669, Oct. 2004.

[3] M. Fujita, K. Wakabayashi, K. Nakada, and K. Kusakabe, "Peculiar localized state at zigzag graphite edge," *J. Phys. Soc. Jpn*., vol. 65, no. 7, pp. 1920-1923, Jul. 1996.

[4] G. Liang, N. Neophytou, D.E. Nikonov, and M.S. Lundstrom, "Performance projections for ballistic graphene nanoribbon field-effect transistors," *IEEE Trans. on Electron Devices*, vol. 54, no. 4, pp. 677-682, Apr. 2007.

[5] M.Y. Han, B. Özyilmaz, Y. Zhang, and P. Kim, "Energy band-gap engineering of graphene nanoribbons," *Phys. Rev. Lett*., vol. 98, no. 20, p. 206805, May 2007.

[6] X. Li, X. Wang, L. Zhang, S. Lee, and H. Dai, "Chemically derived, ultrasmooth graphene nanoribbon semiconductors," *Science*, vol. 319, pp. 1229-1232, Feb. 2008.

[7] Y.W. Son, M.L. Cohen, and S.G. Louie, "Energy gaps in graphene nanoribbons," *Phys. Rev. Lett*., vol. 97, no. 21, p. 216803, Nov. 2006.

[8] H. Min, B. Sahu, S.K. Banerjee, and A.H. MacDonald, "*Ab initio* theory of gate induced gaps in graphene bilayers," *Phys. Rev. B*, vol. 75, no. 15, p. 155115, Apr. 2007.

[9] H. Hosokawa, H. Ando, and H. Tsuchiya, "Performance potentials of bilayer graphene and graphene nanoribbon FETs," to be presented at *Int. Conf. Solid State Devices and Mater*. (*SSDM*'10), Tokyo, Japan, Sep. 2010.

[10] D. Gunlycke and C.T. White, "Tight-binding energy dispersions of armchair-edge graphene nanostrips," *Phys. Rev. B*, vol. 77, no. 11, p. 115116, Mar. 2008.

[11] P. Zhao, J. Chauhan, and J. Guo, "Computational study of tunneling transistor based on graphene nanoribbon," *Nano Lett*., vol. 9, no. 2, pp. 684-688, 2009.

[12] A. Rahman, J. Guo, S. Datta, and M.S. Lundstrom, "Theory of ballistic nanotransistors," *IEEE Trans. on Electron Devices*, vol. 50, no. 9, pp. 1853-1864, Sep. 2003.

[13] Y. Ouyang, Y. Yoon, and J. Guo, "Edge chemistry engineering of graphene nanoribbon transistors: A computational study," in *IEDM Tech. Dig*., 2008, pp. 517-520.

[14] Y. Ouyang, Y. Yoon, J. K. Fodor, and J. Guo, "Comparison of performance limits for carbon nanoribbon and carbon nanotube transistors," *Appl. Phys. Lett*., vol. 89, no. 20, 203107, 2006.

[15] H. Tsuchiya, H. Ando, S. Sawamoto, T. Maegawa, T. Hara, H. Yao, and M. Ogawa, "Comparisons of performance potentials of silicon nanowire and graphene nanoribbon MOSFETs considering first-principles bandstructure effects," *IEEE Trans. on Electron Devices*, vol. 57, no. 2, pp. 406-414, Feb. 2010.

[16] A. Paul, S. Mehrotra, G. Klimeck, and M. Luisier, "On the validity of the top of the barrier quantum transport model for ballistic nanowire MOSFETs," in Proceedings of *IWCE* (International Workshop on Computational Electronics), Beijing, 2009, pp. 173-176.

[17] J. Guo, A. Javey, H. Dai, and M. Lundstrom, "Performance analysis and design optimization of near ballistic carbon nanotube field-effect transistors," in *IEDM Tech. Dig.*, 2004, pp. 703-706.